

PAPER • OPEN ACCESS

Light trapping effect of textured FTO in perovskite solar cells

To cite this article: J F Li *et al* 2019 *IOP Conf. Ser.: Mater. Sci. Eng.* **479** 012046

View the [article online](#) for updates and enhancements.



IOP | ebooks™

Bringing you innovative digital publishing with leading voices to create your essential collection of books in STEM research.

Start exploring the collection - download the first chapter of every title for free.

Light trapping effect of textured FTO in perovskite solar cells

J F Li, H Y Hao¹, J B Hao, L Shi, J J Dong, H Liu and J Xing

School of Science, China University of Geosciences, Beijing, 100083, China

¹ E-mail: huiyinghaol@cugb.edu.cn

Abstract. Hybrid organic–inorganic halide perovskites solar cells (PVSCs) have made great progress in just a few years. With maximum efficiencies evolving from 3.8% to 22.1%. The ongoing efficiency improvements are obtained mainly through the optimization of material process and the enhancement of interface. Whereas the conflict between generating photo carriers and collecting carriers is still a challenge for PVSCs. Light trapping design provides a promising way to solve the problem. However, there are few reports about light trapping effect in PVSCs. In this contribution, FTO substrates with different texture etched by laser were used to fabricate PVSCs. The influence of roughness on absorption of the perovskites layer and extraction properties of the carriers across the interface were discussed. The results showed that the device on the FTO substrate etched by laser with 4A current intensity showed a highest power conversion efficiency, with an enhancement of 13.2% compared with that on the unetched substrate due to the improved scattering of light in the photoactive layer. Our result is expected to open up a new way to enhance the PCE of PVSCs.

1. Introduction

In the past few years, hybrid organic–inorganic halide perovskites have been one of the hottest topics in the field of photovoltaics due to their unique physical and chemical characteristics, long carrier diffusion length, controllable band gap and excellent absorbance [1-3]. The perovskite solar cells (PSCs) made remarkable progress with maximum power conversion efficiencies evolving from 3.8% in 2009 to a certified 22.1% in 2016 [4-11]. The ongoing efficiency improvements are obtained mainly through the optimization of perovskite preparation recipes and process, the enhancement of interface quality and degradation mitigation [12]. Moreover, different device configurations were developed, including the original mesoporous n-i-p junction and mesoporous-free planar junction which involves both n-i-p and p-i-n configuration. Although impressive progress has been made, challenges for PSCs still exist. One of the problems is the conflict between generating photo carriers and collecting carriers. It is widely accepted that the thickness of the perovskite layer should be less than the diffusion length of carriers for efficient extraction, whereas the reduced perovskite material will definitely lead to insufficient light absorption, which means the number of photocarriers decrease [13]. To solve the problem, light trapping design is a promising way, because the optical optimization can achieve the effect of "electrical thin" and "optical thickness" [14-15]. Generally, there are two common ways to develop the trapping effect. One is the light scattering method, and the other is to enhance the surface plasmon resonance effect [16-18]. In this paper, based on the method of silicon thin film solar cells in recent years [19-21], five kinds of FTO substrates with different textures are obtained from the substrate angle of the PVSCs, and the commercial fluorine doped tin oxide (FTO) is used on the basis of different current intensity laser etching. By increasing the contact area of the perovskite layer and



the charge collection layer, the light scattering is enhanced and the optical path is extended to achieve the trapping effect in PVSCs [22].

2. Experimental section

2.1. Substrates preparation

Five kinds of FTO glass were used as substrates for preparation of perovskite solar cell. The a-FTO (Pilkinton) is original commercial substrate which has not been etched by laser. While b-FTO, c-FTO, d-FTO and e-FTO are the etched substrates by laser with power of 4.8W, 5.4W, 6W and 6.6W, respectively.

2.2. Device fabrication

For the fabrication of perovskite solar cells, firstly, the FTO substrates were cleaned in acetone, isopropanol and ethanol, deionized water sequentially for 15 min. The compact TiO₂ was spin-coated on FTO substrates with spinning speed was 3000rpm for 30 s following by annealing at 150 °C for 15 min in air and subsequently sintering at 500 °C for 30 min. After cooling to room temperature, the substrates were immersed in 40mM TiCl₄ solution (48ml DI water and 2ml TiCl₄) at 70 °C for 30 min and sintered at 500 °C for 30 min. Secondly, mesoporous TiO₂ layer was spin-coated at 5000rpm/40s following by annealing at 80 °C for 40 min, and then immersing 20mM TiCl₄ solution (49ml DI water and 1ml TiCl₄) at 70 °C for 30 min, finally sintered at 500 °C for 30 min. 1M lead iodide (PbI₂) solution in dimethylformamide (DMF) was dropped on the TiO₂/FTO substrates by spin-coating at 3000 rpm for 30s, and then dried on a hot plate at 70 °C for 15 min. After cooling, methylamine iodine (CH₃NH₃I) of 50mg/ml was spin-coated at 4000rpm for 40s and then annealed at 100 °C on a hot plate for 30 min. The Spiro-OMeTAD (73.2 mg Spiro, 1mL chlorobenzene, 28 μL TBP and 17μL lithium salt mixed) layer was stirred outside and then spin-coated on the perovskite film at 2000 rpm/40 s. Finally, the silver counter electrode of 100 nm thickness was deposited on the top of the device using thermal evaporation.

2.3. Film and device characterization

Sample morphology of perovskite films were characterized using a scanning electron microscope (SEM) (Hitachi S-4800). The root mean square (RMS) roughness of substrates prepared by laser current strength etching were carried out by atomic force microscopy (AFM) (Bruker Dimension Icon). The diffuse transmittance and transmittance spectra of different substrates were measured with UV-Vis-NIR spectrophotometer (Cary 5000). The basic properties of different FTO substrates were measured by HALL SYSTEM (HL5500). The steady state photoluminescence (PL) spectroscopy was measured with a PL spectrometer (FluoroMax-4), and a pulsed laser with a wavelength of 510 nm with repetition rate of 1 MHz. Photocurrent density-voltage (J-V) curves of solar cells were measured at room temperature with a power source meter (Keithley 2400), and the scanning direction is from positive bias at 1.2 V to 0 V with a delay time of 0.02s for each measurement point. A solar simulator (Zolix ss150) with compact xenon light source was used to produce the simulated AM 1.5G irradiation (100 mW/cm²), and the calibration of the light was carried out by a detector (SOFN INSTRUMENTS CO 110#-1400225-3) with silicon reference cell.

3. Result and discussion

3.1. Substrates properties

The surface morphology and root mean square (RMS) roughness of different etching substrates are recorded by AFM in Figure 1. It is obviously observed that the grain size and roughness of different FTO substrates as shown in Figure 1. a, b, c, d, e. Compared with the original commercial a-FTO, the grain size and surface roughness of b-FTO (4A) is one of the largest, which is pivotal for the continuous surface morphology of compact TiO₂ layer, mesoporous TiO₂ layer and perovskite films.

With the laser etching current intensity and the etching power increase, the surface texture becomes less obvious, and the grain size and surface roughness of c-FTO (4.5A), d-FTO (5A), e-FTO (5.5A) decreased in turn. The specific surface roughness of five different substrates is shown in Table 1.

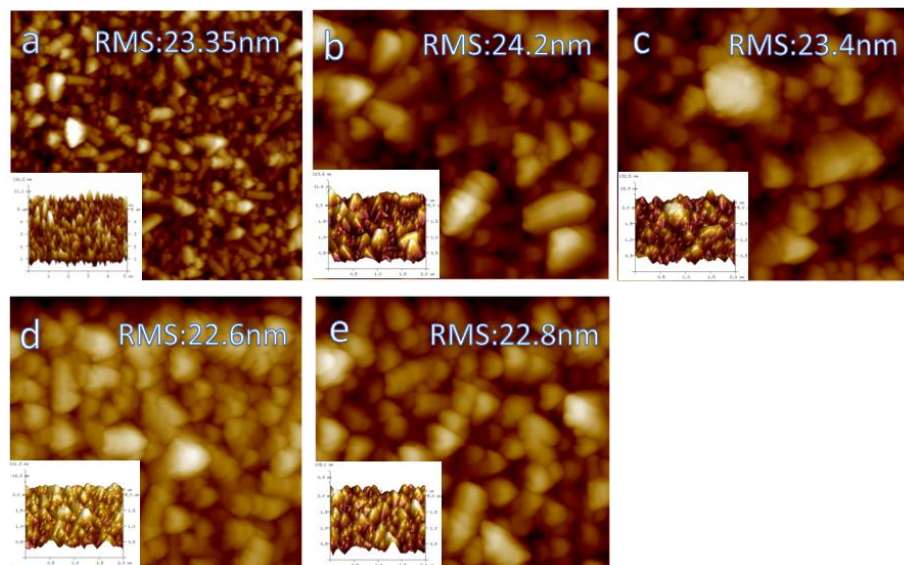


Figure 1. Morphologies and roughness of different FTO substrates. Surface morphology and average roughness of a-FTO (original), b-FTO (4A), c-FTO (4.5A), d-FTO (5A) and e-FTO (5.5A) in (a), (b), (c), (d), (e).

The transmittance (T_d) and transmittance (T) spectra of different substrates were measured with UV-Vis-NIR spectrophotometer in Figure 2. As can be seen from Figure 2a and b, the transmittance of the five FTO substrates is higher, the transmittance of A-FTO is close to 80% at wavelength of 300-1000nm, and the FTO transmittance of different power etching is reduced. At the same time, the haze of FTO substrates with different power etching is calculated by using formula (1), it is the difference between the diffuse transmittance (T_d) and transmittance (T) divided by the the diffuse transmittance (T_d).

$$Haze = \frac{T_d - T}{T_d} \times 100\% \quad (1)$$

The haze of FTO increased by laser etching compared with the original FTO in Figure 2c. From the above experimental data, the transmittance of the original FTO is higher than that of the FTO substrates treated by the laser etching of different power. The haze of FTO will play a very positive role in short circuit current density due to the effect of the light trapping in the PVSCs. With the increase of laser etching intensity, the square resistance of FTO substrate also increases and the FTO film becomes thinner. The square resistance of a-FTO is 7.68 Ω/sq . When the laser is etched, the resistance of b-FTO, c-FTO, d-FTO, e-FTO increase to 22.05, 31.02, 40.81, 48.37 Ω/sq . Therefore, b-FTO (4A) has the suitable characteristics to improve the performance of perovskite solar cells.

Table 1. The basic properties of five laser current intensity etched FTO substrates.

Test parameters	a-FTO (original)	b-FTO (4A)	c-FTO (4.5A)	d-FTO (5A)	e-FTO (5.5A)
RMS(nm)	23.35	24.2	23.4	22.6	22.8
$R_{sq}(\Omega/\text{sq})$	7.68	22.05	31.02	48.56	59.14
Mobility($\text{cm}^2/\text{V s}$)	4.5	4.49	2.9	2.74	1.98
Carrier concentration(cm^{-3})	$-1.81e^{+17}$	$-6.31e^{+16}$	$-6.93e^{+16}$	$-4.70e^{+16}$	$-5.32e^{+16}$

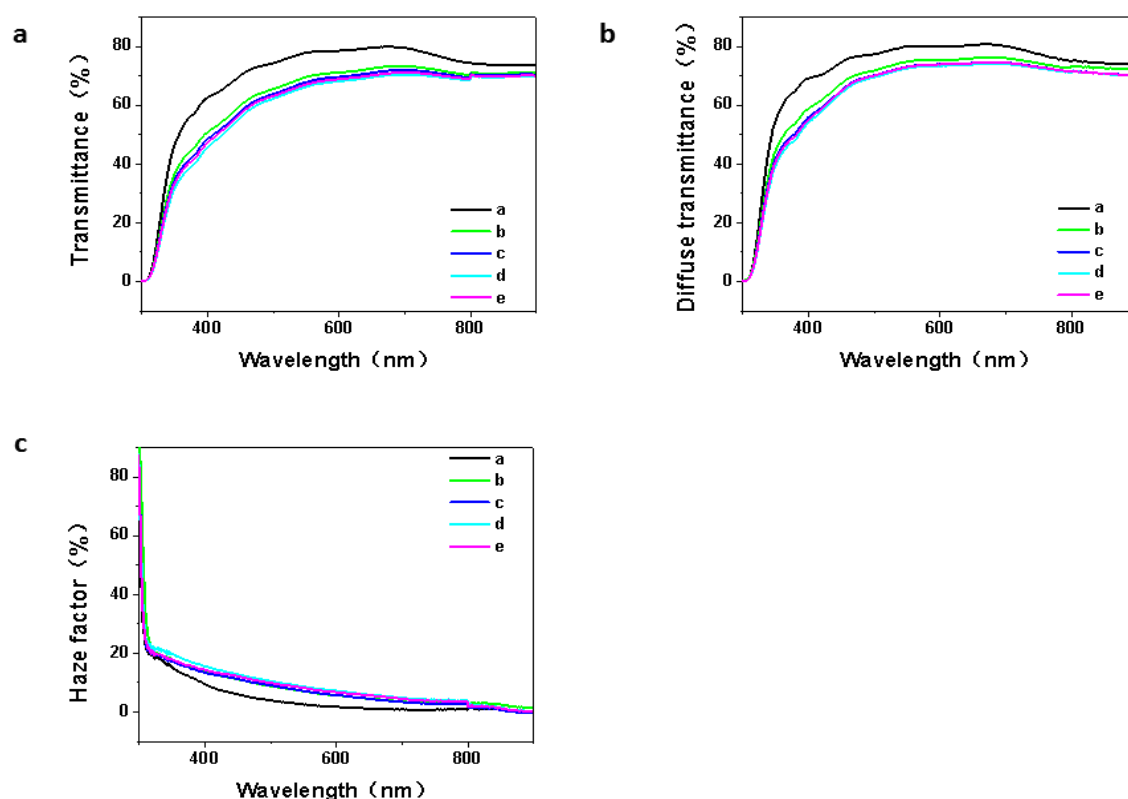


Figure 2. Transmittance spectra , diffuse transmittance spectra and haze factor of a-FTO (original), b-FTO (4A), c-FTO (4.5A), d-FTO (5A) and e-FTO (5.5A) in (a), (b), (c).

3.2. Film growth and properties

In order to further discuss the effect of textured substrates on the perovskite films and devices, the PVSCs with a structure of FTO/compact TiO_2 /mesoporous TiO_2 / $\text{CH}_3\text{NH}_3\text{PbI}_3$ /Spiro-OMeTAD/Ag were prepared in this work. Meanwhile, the properties of the perovskite layer and devices were also investigated. As is shown in Figure 3, SEM images of perovskite films of a-FTO (original), b-FTO (4A), c-FTO (4.5A), d-FTO (5A) and e-FTO (5.5A) in a, b, c, d, e. The $\text{CH}_3\text{NH}_3\text{PbI}_3$ Film Prepared on b-FTO have larger grain size less grain boundary than that of other FTO substrates, which is consistent with the previous AFM diagram of different FTO substrates. It can prove that the textured FTO substrates of b-FTO contributes to the growth of the perovskite film.

Figure 4a and b are the transmission and absorption spectra of $\text{TiO}_2/\text{CH}_3\text{NH}_3\text{PbI}_3$ thin films prepared on five kinds of FTO. It can be seen that the $\text{TiO}_2/\text{CH}_3\text{NH}_3\text{PbI}_3$ prepared on the FTO substrate with the laser treatment has a lower absorption in the wavelength range of 500-600nm. However, the absorption shows a higher absorption at the wavelength range of 600-800 nm than that of the untreated FTO substrate. Therefore, the textured substrates helped to enhance the light trapping effect.

Steady state PL spectra was applied to study the charge transfer properties of $\text{TiO}_2/\text{CH}_3\text{NH}_3\text{PbI}_3$ on various FTO. As illustrated in Figure 5. The measurements show that the intensity of the emission peak on b-FTO at 770 nm was drastically reduced owing to the c- TiO_2 /m- TiO_2 quenches the perovskite steady-state PL, suggesting that the better excitation separation at the TiO_2 /perovskite interface. Therefore, the textured b-FTO substrates is helpful for the improvements of charge generation and collection. Moreover, the slight shift of PL peak positions of the five samples may be due to the different defects of the five FTO.

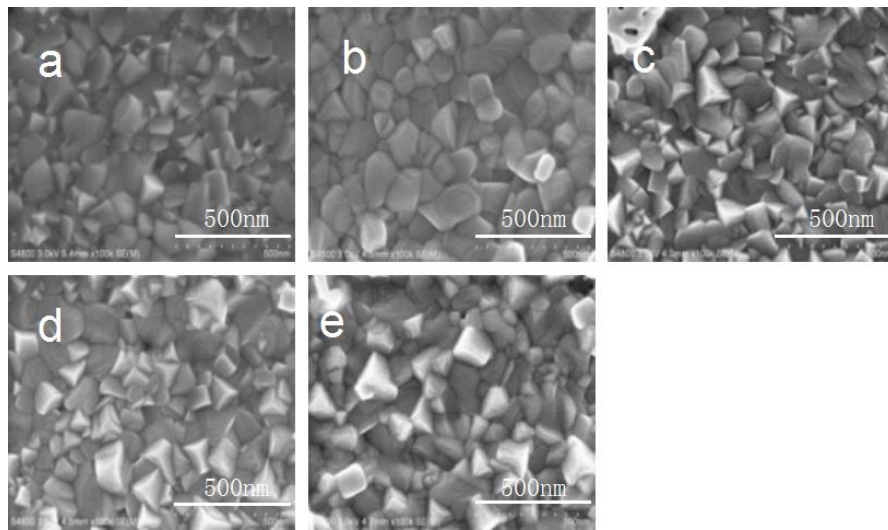


Figure 3. SEM images of perovskite films of a-FTO (original), b-FTO (4A), c-FTO(4.5A), d-FTO (5A) and e-FTO (5.5A) in (a), (b), (c), (d), (e).

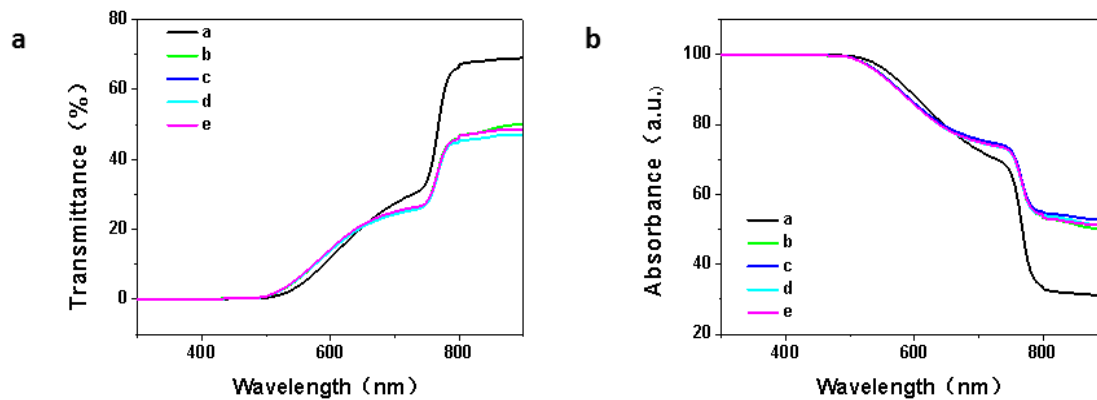


Figure 4. Transmittance and absorbance spectrum of $\text{TiO}_2/\text{CH}_3\text{NH}_3\text{PbI}_3$ on a-FTO (original), b-FTO (4A), c-FTO (4.5A), d-FTO (5A) and e-FTO (5.5A) in (a) and (b).

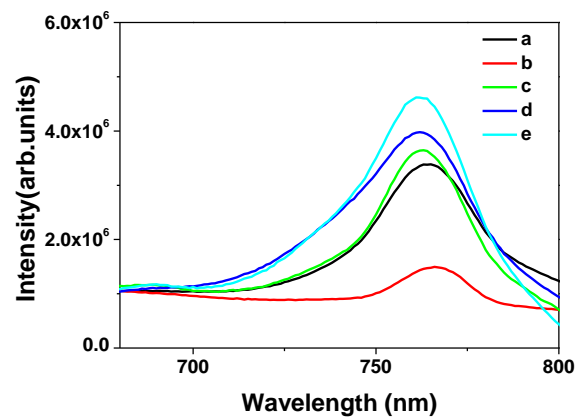


Figure 5. Steady state PL spectra of $\text{TiO}_2/\text{CH}_3\text{NH}_3\text{PbI}_3$ on a-FTO (original), b-FTO (4A), c-FTO (4.5A), d-FTO (5A) and e-FTO (5.5A).

The J-V curves and distribution histogram of PCE of the PVSCs with five kinds of FTO substrates are shown in Figure 6a, b. The corresponding specific photovoltaic performance parameters are listed in Table 2, which indicate that the J_{sc} of PVSCs increases first and then decreases with the increase of laser etching intensity. The PCE and J_{sc} of the b-FTO substrate that was treated by the current intensity of 4A laser etching are 11.34% and 23.97 mA/cm^2 , achieving a 13.17% and 4.76% increase compared to the FTO without laser etching. However, as the laser etching intensity increases, the performance of the device decreases gradually due to the change of the substrate characteristics. Figure 6b shows that more than half of the PSC devices have a PCE over 8% and all of the PSC devices have a PCE over 6%. The average PCE of the 8 PVSCs devices is 10.39%, which indicates a good reproducibility.

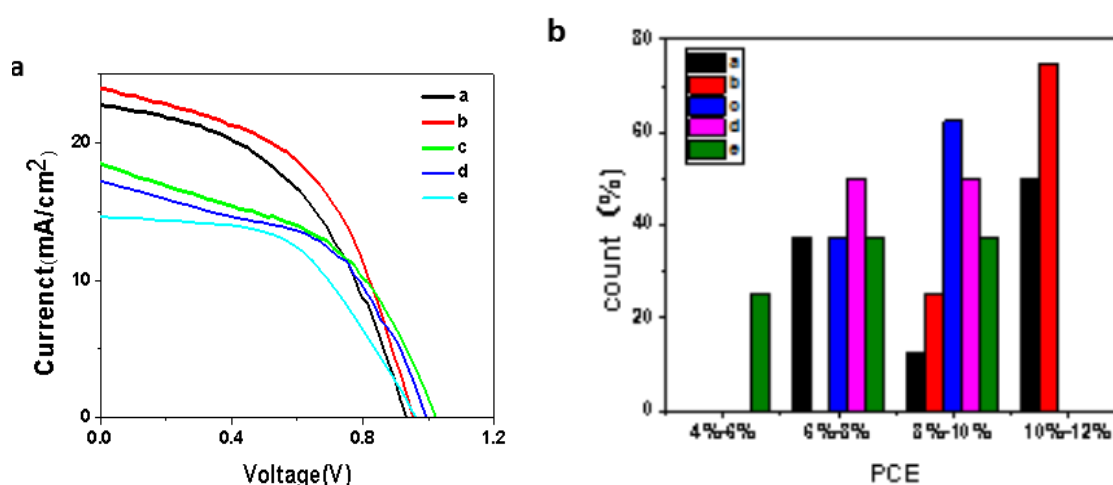


Figure 6. J-V characteristics of devices and distribution histogram of PCE with five FTO substrates in (a), (b).

Table 2. The performance of perovskite solar cells prepared by five kinds of FTO substrates.

Test parameters	a-FTO (original)	b-FTO (4A)	c-FTO (4.5A)	d-FTO (5A)	e-FTO (5.5A)
J_{sc} (mA/cm ²)	22.88	23.97	18.60	17.36	14.64
V_{oc} (V)	0.93	0.95	1.03	0.99	0.97
FF (%)	47	49	46	50	52
PCE (%)	10.02	11.34	8.88	8.60	7.45

4. Conclusions

In summary, we have used a simple and effective method to achieve the light trapping for PVSCs. The results show that the proper laser etching current intensity can help to increase the surface roughness and haze of FTO substrates. Thus, perovskite thin films quality with large grain size has been improved, which is beneficial for the efficiency improvement of perovskite solar cells. The device with textured substrates treated by the current intensity of 4A laser etching achieved an improvement of 13.17% over that of the device without laser etching. Therefore, the light trapping is a feasible method to achieve high efficiencies for PVSCs.

Acknowledgments

This work is supported by the Fundamental Research Funds for the Central Universities under Grand Nos. 2652017163 and 2652017154.

References

- [1] Yella A, Heiniger L P, Gao P, Nazeeruddin M K 2014 *Nano Lett.* **14** 2591
- [2] Eperon G E, Stranks S D, Menelaou C, Johnston M B, Herz L M, Snaith H J 2014 *Energy Environ. Sci.* **7** 982
- [3] Dong Q, Fang Y, Shao Y, Mulligan P, Qiu J, Cao L, Huang J 2015 *Science* **347** 967
- [4] Correbaena J P, Abate A, Saliba M, Tress W, Jacobsson T J, Gratzelc M, Hagfeldt A 2017 *Energy & Environmental Science* **10** 710
- [5] Yang W S, Noh J H, Jeon N J, Kim Y C, Ryu S, Seo J, Seok S I 2015 *Science* **348** 1234
- [6] Jung H S, Park N G 2015 *Small* **11** 10
- [7] Bi D, Yi C, Luo J, Décoppet J D, Zhang F, Zakeeruddin S M, Li X, Hagfeldt A, Grätzel M, 2016 *Nat. Energy* **1** 142
- [8] Kim H S, Lee C R, Im J H, Lee K B, Moehl T, Marchioro A, Moon S J, Humphry-Baker R, Yum J H, Moser J E 2012 *Sci. Rep.* **2** 591
- [9] Kojima A, Teshima K, Shirai Y, Miyasaka T 2009 *J. Am. Chem. Soc.* **131** 6050
- [10] Jeon N J, Noh J H, Yang W S, Kim Y C, Ryu S, Seo J, Seok S I 2015 *Nature* **517** 476
- [11] Zhou H, Chen Q, Li G, Luo S, Song T B, Duan H S, Hong Z, You J, Liu Y, Yang Y 2014 *Science* **345** 542
- [12] Soldera M, Taretto K 2018 *Physica Status Solidi* **1700906** 1
- [13] Lin Q, Armin A, Nagiri R C R, Burn P L, Meredith P 2014 *Nat. Photonics* **9** 106
- [14] Hsu C, Battaglia C, Pahud C, Ruan Z, Haug F, Fan S, Ballif C, Cui Y 2012 *Adv. Energy Mater.* **2** 628
- [15] Lee S, Choi H, Li H, Ji K, Nam S, Choi J, Ahn S, Lee H, Park B 2014 *Sol. Energy Mater. Sol. Cells* **120** 412
- [16] Pala R, White J, Barnard E, Liu J, Brongersma M 2009 *Adv. Mater.* **21** 3504
- [17] Long M, Chen Z, Zhang T, Xiao Y, Zeng X, Chen J, Yan K, Xu J 2015 *Nanoscale* **8** 6290
- [18] Müller-Meskamp L, Kim Y, Roch T, Hofmann S, Scholz R, Echardt S, Leo K, Lasagni A 2012 *Adv. Mater.* **24** 906
- [19] Zheng L, Ma Y, Chu S, Wang S, Qu B, Xiao L, Chen Z, Gong Q, Wu Z, Hou X 2014 *Nanoscale* **6** 8171
- [20] Lin G S, Li C Y, Huang K C, Hounq M P 2015 *Materials Chemistry & Physics* **160** 264
- [21] Yu X, Zhang J, Zhang D, Chen L 2017 *Solar Energy* **153** 96
- [22] Lee W, Hwang T, Lee S, Lee S, Lee S Y, Kang J 2015 *Nano Energy* **17** 180